Old Dominion University

ODU Digital Commons

Political Science & Geography Faculty Publications

Political Science & Geography

9-2001

Spectral Response and Spatial Pattern of Fraser Fir Mortality and Regeneration, Great Smoky Mountains, USA

Thomas R. Allen

Spectral response and spatial pattern of Fraser fir mortality and regeneration, Great Smoky Mountains, USA

Thomas R. Allen[1] & John A. Kupfer[2]

[1]*Department of Political Science and Geography, Old Dominion University, Norfolk, VA, USA (e-mail: tallen@odu.edu);* [2]*Department of Geography and Regional Development, University of Arizona, Tucson, AZ, USA*

Abstract

High elevation Fraser fir (*Abies fraseri*) forests of the Southern Appalachians have undergone widespread mortality since the introduction of the balsam woolly adelgid in the 1950s. Resulting changes in ecosystem pattern and process (e.g., stand dynamic processes) have greatly affected floral and faunal communities. In this project, we integrated field observations, geographic information system topographic models, and 1988–1998 satellite imagery to analyze spatial and temporal conditions of Fraser fir and spruce-fir ecosystems in Great Smoky Mountains National Park. Tasseled cap indices (brightness, greenness, and wetness) and associated spectral changes for Landsat TM digital data were statistically modeled by topographic variables. Spectral changes were recorded using change vector analysis (CVA) and spherical geometry at multiple scales: individual sites, local ridges, and across the east-west gradient of the study area. Significant relationships were found between elevation and observed spectral changes and among mountain sites representing the east-west chronosequence of adelgid infestation. Topographic derivatives were related to tasseled cap and CVA measures in summary statistics, regression, and correlation analysis, revealing significantly different mortality and regeneration pathways that were a function of topographic settings. Geographic variations of these vectors also detail the scope of east-west and localized upslope progression of fir mortality. The application of CVA provided the ability to summarize variation in spectral changes (magnitude and direction) and to ascribe measures to mortality and regeneration processes.

Introduction

Insect outbreaks and infestations are critical events that reshape the composition, structure and function of forest ecosystems. Mortality resulting from an outbreak affects stand dynamic processes, nutrient cycling, trophic relationships, and fire risk and intensity (e.g., Hadley & Veblen 1993; Jenkins et al. 1999), and outbreaks may have long-lasting impacts on ecosystem composition and function (Swetnam & Lynch 1993). While periodic insect outbreaks are a natural component of the disturbance regime in many ecosystems, the introduction of exotic insect pests may be devastating to ecosystems where outbreaks are uncommon phenomena. In such cases, invasions may lead to sufficiently significant alterations in ecosystem processes that recovery to predisturbance conditions is prolonged or even prevented (e.g., Orwig & Foster 1998). Resource managers and ecologists thus recognize the need to measure, monitor and (when possible) model the response of forest ecosystems to outbreaks.

Remote sensing techniques have been used to detect changes in forest health, estimate levels of defoliation and mortality, and map the extent and spread of damage due to insect pests (e.g., Nelson 1983; Buchheim et al. 1985; Mukai et al. 1987; Joria et al. 1991; Brockhaus et al. 1992; Franklin & Raske 1994; Royle & Lathrop 1997; Radeloff et al. 1999). The detection, mapping and monitoring of outbreaks using satellite imagery is based on change detection techniques that

are applicable to a broad range of applications, including image differencing, principal components analysis, spectral change classification, post-classification change differencing and change vector analysis (Rock et al. 1986; Muchoney & Haack 1994; Collins & Woodcock 1994, 1996; Allen & Kupfer 2000). Even though insect defoliation has been a major application within the field of change detection research, classifications of defoliation have been only moderately successful, and there continues to be a need to improve change detection techniques (Radeloff et al. 1999). Further, relatively few studies have coupled remote sensing and geographic information systems to assist in the development of models of forest vulnerability (e.g., Luther et al. 1997) or to relate patterns of defoliation, forest mortality or understory regeneration to abiotic or biotic factors (e.g., McCullough et al. 1996; Bonneau et al. 1999; Allen & Kupfer 2000). The latter, in particular, would permit a better understanding of the initiation, spread and short- to long-term consequences of outbreaks.

Study objective

High elevation Fraser fir (*Abies fraseri*) and Fraser fir-red spruce (*Picea rubens*) ecosystems in the southern Appalachians are among the most rare and endangered ecosystem types in the United States (Noss et al. 1995). Much of the concern about the future of these ecosystems stems from massive Fraser fir dieback following the introduction of a Eurasian insect, the balsam woolly adelgid, in the 1950s (e.g., Balch et al. 1964). In the Smoky Mountains (TN/NC), which contain roughly 75% of all southern spruce-fir ecosystems, mortality rates of mature fir surpassed 90–99% following the introduction of the adelgid, leading to significant declines in basal area and canopy cover and attendant problems for faunal communities (Alsop & Laughlin 1991; Nicholas et al. 1992; Rabenold et al. 1998: Nicholas et al. 1999). While there are some areas of vigorous fir reproduction beneath the dead fir canopy, the understory in many other locations has been invaded by a mix of herbaceous and deciduous woody species (DeSelm & Boner 1984; Pauley & Clebsch 1990). The underlying causes of these differing regeneration patterns across the landscape, if any, have not been examined in detail, and the long-term fate of Fraser fir ecosystems continues to be questionable (Nicholas et al. 1999; Smith and Nicholas 2000).

The goal of this paper is to examine vegetation patterns in high elevation conifer forests in Great Smoky Mountains National Park using satellite images from 1988 and 1998. We hypothesize that current patterns of vegetation in spruce-fir and 'pure' fir ecosystems reflect spatial variability in:
  – the predisturbance patterns of Fraser fir occurrence (e.g., the amount of fir vs. non-fir individuals),
  – the timing of adelgid arrival and fir mortality (and thus the amount of time the site has had to recover), and
  – the subsequent understory responses to abiotic conditions.

With respect to these three points, we hypothesize that spatial patterns of mortality and regeneration should be related to patterns of abiotic factors because:
  – predisturbance patterns of fir abundance were related to elevational gradients in temperature and moisture (Busing et al. 1993),
  – the dispersal of adelgids by wind and their subsequent deposition may have been related to topographic factors (e.g., Hay et al. 1978), and
  – regeneration should be associated with microclimatic and microtopographic variables (cf., Kupfer et al., in review).

To test these hypotheses, we analyzed spectral reflectance from Landsat Thematic Mapper (TM) images. We first related tasseled cap measures of reflectance (brightness, greenness, wetness) from 192 forest plots to levels of canopy closure and understory composition. Once we established that tasseled cap values could be tied to differences in overstory and understory condition, we tested for statistical relationships between six mortality/regeneration classes and environmental factors in an effort to better understand the controls over mortality and regeneration patterns. As part of the analysis, we applied an improved change vector analysis technique (cf., Allen & Kupfer 2000) to summarize the magnitude and direction of change of tasseled cap indices for the forest plots from 1988–1998. By including change variables in our analyses, we could thus examine relationships not only between forest characteristics and abiotic conditions for a given image, but also test the hypothesis that sites with similar abiotic characteristics displayed similar responses to the introduction of the adelgid.

Methodology

Study site

The study was conducted at Great Smoky Mountains National Park (GSMNP), USA. Elevation within the Park ranges from 400–2015 m, and vegetation patterns reflect the influence of environmental gradients tied to elevation and topography (Whittaker 1956) as well as the effects of human disturbance, including agriculture and logging (Pyle 1985). Prior to the introduction of the adelgid, stands from ca. 1500–1800 m were dominated by red spruce with a smaller component of Fraser fir and yellow birch (*Betula lenta*). Fraser fir increased in importance with elevation and was found in nearly pure stands along the crest of the Smokies above 1890 m (Busing et al. 1993). The death of most mature fir in the fir zone, however, has left behind a mosaic of sites representing various successional stages and pathways.

We focused our analyses on five of the highest peaks within GSMNP: Clingmans Dome, Mt. Guyot, Mt. LeConte, Mt. Kephart, and Mt. Collins. Previous research has shown that the adelgid was originally introduced into the eastern part of the park and dispersed westward (Hay et al. 1978). Mortality rates peaked in the eastern third of our study area (Mt. Guyot) in the 1970s, in the central region (Mt. LeConte, Mt. Kephart) in the early 1980s, and in the western region (Mt. Collins, Clingmans Dome) from the mid-1980s through the 1990s, although the local timing of peak mortality varied with elevation (Smith & Nicholas 1998). Adelgid infestations on most peaks initially occurred at the lower elevations of the spruce-fir forest type and spread upslope. Fir forests at GSMNP thus constitute east-west and downslope-upslope chronosequences of infestation and recovery (Smith & Nicholas 1998).

Data acquisition and preprocessing

Two Landsat TM scenes (18 August 1988, 15 September 1998) were used to investigate spruce-fir forest change via tasseled cap transform and change vector analysis (CVA). In our selection of the specific image dates, we considered the replication of illumination conditions and sufficient time of forest change. Late summer (mid-August to mid-September) was the most opportune time for image acquisition with the additional benefit that understory vegetation, ground cover, and sub-canopy foliage may have less spectral influence at this time (Ekstrand 1989). However, because of the temperate rainforest conditions of the Smoky Mountains, cloud-free Landsat Thematic Mapper imagery within the seasonal window was available only for years 1988, 1989, and 1998. Additional data used for this study included US Geological Survey 1:24 000 digital elevation models (DEMs), the location and degree of adelgid infestations circa the mid-1970s as approximated from field surveys and aerial photography (Hay et al. 1978), and GIS coverages of park disturbance history (Pyle 1985).

The summer abundance of aerosols and particulates in the Great Smoky Mountains necessitated the application of atmospheric correction and radiometric normalization for conditions of the two image dates. Normalization of the images ensured that changes extracted between dates would represent actual ground changes and not merely atmospheric or other exogenous factors resulting from illumination or sun-target-satellite geometry. Ground control points were obtained from differentially-corrected GPS positions using map and image file coordinates for both normalization and subsequent field plots. GPS rover positions were taken using a Topcon Turbo-G1 receiver with an external high-gain, multipath-resistant antenna and corrected using base station data. The 15 September 1998 Landsat TM scene was selected as the reference to which the 18 August 1988 image was normalized using the general approach of Hall et al. (1991). *In situ* ground data on the position, cover, and surface materials were collected two weeks prior to the 1998 image acquisition.

To normalize the images, we applied linear regressions to predict a brightness value in each band for the 1988 image. Normalization targets were selected for stable reflectance characteristics using an approach similar to Jensen et al. (1995). Following the approach of Yuan & Elvidge (1996), we sought pixels that did not change spectrally between the image dates (e.g., large rock outcrops, stable lakes). Normalization targets were selected in relatively flat, low elevation locations to minimize topographic and residual atmospheric bias (cf., Eckhardt et al. 1990). Low brightness targets were located in deep reservoirs while dry targets included rock outcroppings and large roadways along the Newfound Gap Road. Paved asphalt features provided additional pseudo-invariant targets (Hall et al. 1991). In all, twenty-nine targets were used for both dates. The slopes associated with the regressions (all significant $p < 0.0001$) were moderate and accounted for the residual atmospheric, sun

angle, and moisture conditions in the remotely sensed data.

Topographic normalization techniques were applied in an attempt to reduce bias of reflectance in features owing to illumination (aspect and slope-induced reflectance variations). Initial attempts indicated strong correlations when using forested pixel locations from a wide topographic range; however, the coefficients were found to be insignificant ($\alpha = 0.05$) when applied only to high elevation (> 1800 m) sites in this region. Thus, although the effects of topographic bias can have a major influence on spectral-topographic relationships in Landsat data, the effects for the spruce-fir zone examined in this study were believed to be negligible.

Derivation of tasseled cap indices and terrain variables

Tasseled cap transformations are linear combinations of original Landsat bands that allow for data compression through three descriptive indices (brightness, greenness, and wetness bands). These indices can provide for improved interpretation of biophysical characteristics for agricultural and ecological applications and can facilitate more straightforward change detection in forest ecological analyses. (Crist & Cicone 1984). The brightness index is positively correlated with soil reflectance and has been used to determine soil characteristics; the greenness index is positively correlated with the total amount of green vegetation and has been used to determine green canopy characteristics, and the wetness index is positively correlated with canopy and soil moisture and has been used to determine full canopy closure achievement and the relative mixture of vegetation and soil (Crist & Cicone 1984).

Maps of independent topographic variables, including elevation, slope angle, curvature, summer solar radiation potential and slope position were derived from the DEMs. Curvature refers to the shape of the slope and was calculated in planform and profile index for rook's case neighbors (continuous scale: -1: concave, 0: flat, $+1$: convex). Solar radiation potential was estimated by a model that aggregated and rescaled direct beam insolation calculated from the DEM without adjustment for indirect/diffuse sky or terrain irradiance. The model simulated summer insolation over three months, providing an index of available photosynthetic radiation that was primarily a function of slope aspect and angle. Slope position was

calculated using an index that quantifies upslope pixel flow accumulation and re-scales this by the distance from drainage divide (lower values: ridge sites; higher values: downslope/cove sites).

The sample design was structured to capture the chronosequences (east-west and downslope-upslope) of adelgid spread. Intensive study sites were selected from the five mountain peaks on the basis of prior field work, ancillary historical notes, and accessibility. For each intensive site, a purposive sample point was selected in the field based on forest cover and structure for a spectral training site and photointerpretive key. Fifty-four sites were thus field-located and fixed with differential GPS post-processing. Additional sites were then randomly selected from the intensive areas and photointerpretated using digital orthophotos and Indian Remote Sensing satellite 5 m panchromatic imagery. A total of 192 sites were selected for which we extracted all spectral and topographic variables.

Change vector analysis

To assess the extent and nature of changes in reflectance patterns for the study sites from 1988–1998, we used change vector analysis (CVA). With CVA, the change in spectral reflectance values (e.g., pixel digital numbers, tasseled cap values) between two or more dates is analyzed using Euclidean geometry. As an example, consider a case with two times (t_1 and t_2) and three different spectral indices: tasseled cap brightness (X_{t1} and X_{t2}), greenness (Y_{t1} and Y_{t2}) and wetness (Z_{t1} and Z_{t2}) (Figure 1a). For a given location (i.e., a specific Landsat TM pixel), a three-dimensional vector, or directed line, can be derived having an origin (value at t_1) and an endpoint (value at t_2)

The *total magnitude of change* (D) between the dates is calculated using three terms in a simple Pythagorean formula:

$$D = \sqrt{(X_{t2} - X_{t1})^2 + (Y_{t2} - Y_{t1})^2 + (Z_{t2} - Z_{t1})^2}.$$

Spherical statistics were used to derive and compare additional change measures for each pixel, including mean vector directions in two planes, the mean resultant vector length and the spherical variance. While specific methods concerning the derivation of these variables is beyond the scope of this paper (see Allen & Kupfer 2000), a brief discussion is worthwhile.

Two direction angles were measured for each vector using trigonometric functions, and the vector direction was measured in polar coordinates (θ, ϕ) for
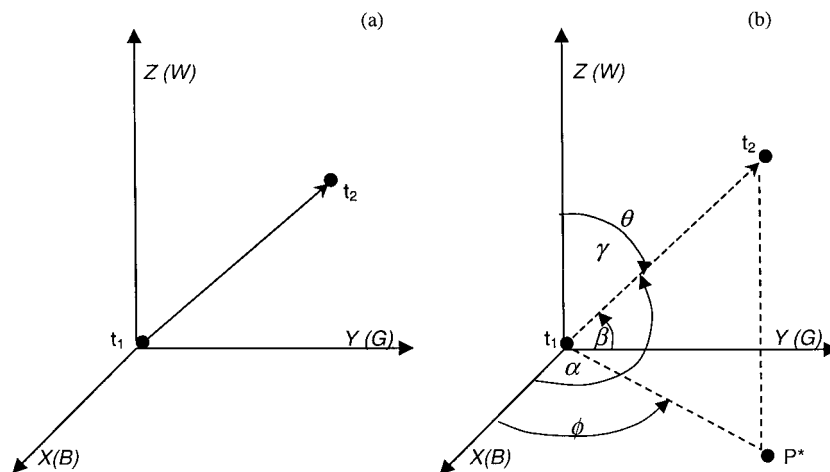
Figure 1. Illustrative diagram of change vector analysis (CVA) for a pixel on two dates. Vector shown in (a) has initial (t_1) and second date (t_2) tasseled cap brightness, greenness, and wetness values along x, y, and z axes, respectively. Vector (b) for another hypothetical pixel illustrates more acute direction angles and a smaller change magnitude. Polar coordinates for CVA direction are shown by colatitude (θ) and colongitude (ϕ), while direction cosines for spherical statistics are given by α, β, γ.

subsequent visualization. The first angle, θ, was measured from the wetness axis (z) toward the greenness axis (y) (or ZY plane); the second, ϕ, was measured from the y (greenness) to x (brightness) direction (or XY plane) (Figure 1b). Further, any given set of pixels belonging to a group (e.g., a vegetation class) will have n unit vectors corresponding to pixels in a sample. Direction cosines for vectors relative to the x, y, and z axes can be summed and squared to give a *resultant vector length* (R) for each group. The *mean resultant vector length* (R/n) is an indicator of vector directionality; higher values indicate groups that have similar vector directions, even if the overall magnitude of change is small. However, symmetric placement of points at endpoints of the vector can result in a value of 0, falsely indicating scatter (cf., Allen & Kupfer 2000). Polar plots and perspective displays are thus intrinsic to the analysis of spherical distributions. Group directional variance and standard deviation can also be calculated. Further guidance in deriving and converting spherical coordinate systems can be found in Fisher et al. (1987) and Fisher (1993).

To apply this methodology, we transformed normalized Landsat TM data using coefficients for Landsat-5 tasseled cap. An algorithm was developed and coded into a graphical modeling script within the image processing software to conduct CVA. The model uses tasseled cap images (brightness, greenness, and wetness) as input and calculates the change magnitude (D) and direction vectors for all pixels. The algorithm then produces three images containing:

– total magnitude D,
– polar coordinates for vectors (θ, ϕ), and
– the direction cosines for vectors relative to x, y, and z axes, which are used to calculate the CVA mean directions and variances. Raw values for output layers were retained without rescaling.

Site selection, vegetation classification, and statistical analyses

From 1998 to 2000, we estimated composition and percent cover (0–100%) for overstory and understory vegetation at a number of field reference sites. Based on composition and cover, the sites were classified using a six-class stratification representative of mortality/canopy cover and regeneration conditions. The classes were exhaustive and mutually exclusive and included an initial three point division:

(A) open canopy condition (>70% canopy open),
(B) thinned canopy condition (10–70% canopy open), and
(C) closed canopy condition (dominated by light flecks and small inter-branch openings). Within these categories, subtypes were defined on the basis of either understory composition (Classes A & B) or overstory dominant (Class C), resulting in six subtypes:

A1 open canopy with fir regeneration dominant;
A2 open canopy with regeneration dominated by deciduous or herbaceous species;
B1 thinned canopy with fir regeneration dominant;

B2 thinned canopy with regeneration dominated by deciduous or herbaceous species;

C1 closed canopy dominated by overstory fir, and

C2 closed canopy dominated by red spruce or a mix of red spruce and yellow birch.

Aerial photointerpretation keys were used to identify photomorphic examples of the six classes in 1997 B/W prints, digital orthophoto quarter-quads and an Indian remote sensing satellite (IRS-1) panchromatic image from April 1998. The data were analyzed in two ways. First, the categories of forest condition (A1, A2, B1, B2, C1, C2) were compared using nonparametric analysis of variance methods to test for differences in their reflectance properties (tasseled cap greenness, brightness, wetness). Vector magnitudes and angles were calculated and graphed in polar plots to permit visual assessment of between-class differences and facilitate hypothesis development concerning regeneration patterns. Polar plots were generated to portray the angular variation in each axis of spectral change and to include the total magnitude as a radius distance for any given point. Pixel CVA values were characterized by symbolizing their field-observed overstory and understory structure and composition. Because plotting of summary change vectors in map form can improve visualization of directional changes in spectral patterns, we subset and summarized the CVA magnitude and directional measures to map their distribution using a vane plot which facilitated graphic representation of multivariable data, including spatial location, in map form.

Second, linear regression models of the statistical relationships between raw tasseled cap index values and topographic variables were generated for each vegetation class and mountain group (Guyot, LeConte/Kephart, Clingmans/Collins). We used these analyses to test for differences in reflectance patterns related to the topographic variables and argue that such correlations should be indicative of their relative role in adelgid-caused mortality and regeneration because of the relationships between spectral properties and the forest classes, as outlined in the first part of our study. We also correlated CVA variables (magnitude, direction) with topographic variables to test for systematic differences in change magnitude and direction that might be related to topographic constraints. The spatial chronosequence at GSMNP was examined by comparing results of the analyses for the eastern site (Mt. Guyot: $n = 29$), central sites (Mt. Kephart/LeConte: $n = 92$), and western sites (Mt. Collins/Clingmans Dome: $n = 71$). Linear statistics

using the angular CVA variables incorporated a linear normalization by rank-ordering the angular variables to reduce bias (cf., circular order statistics, Fisher 1993). Because of the unequal number of sample sites from different mountains and forest classes, we exercised caution in all of our comparisons of statistical coefficients and standard errors.

Results

Relationships between tasseled cap indices and vegetation classes

Results of Kruskal–Wallis nonparametric ANOVA's (used because tasseled cap data failed tests for normality and equality of variances among forest classes) indicated significant differences in mean values of all three tasseled cap indices for both four group (open overstory, thinned overstory, and closed overstory I and II) and six group (including the subdivisions of open and thinned overstory) classifications. Pairwise Mann–Whitney tests delineated a decreasing gradient of brightness values from open overstory stands dominated by fir regeneration to closed-canopy fir stands, with other classes having intermediate values in 1998 (Table 1). Greenness values also differentiated closed canopy fir stands from all other classes. At the four-class level, wetness distinguished open overstory plots (with lower values and drier conditions) from thinned and closed overstory plots (with higher values and wetter conditions). Pairwise comparisons at the six-class level showed that this difference was the result of low wetness values for the open canopy, fir-dominated regeneration class. For the thinned canopy stands, those with fir regeneration had higher wetness values than those with deciduous and herbaceous growth. Closed overstory stands of both types were comparable to thinned stands with deciduous regrowth.

When we examined the temporal patterns of reflectance values using change vector analysis, several additional differences among the vegetation classes were evident. From 1988–1998, the total magnitude of change in tasseled cap values (D) was highest for the open overstory plots, intermediate for thinned plots with a non-fir understory, and lowest for closed canopy plots (Table 2). In terms of directional change, colongitude (ϕ, the brightness-greenness plane) differentiated the thinned sites, particularly those with fir regrowth. Colatitude (θ, the tasseled cap greenness-wetness plane) primarily distinguished closed canopy

Table 1. Mean (± s.e.) values of 1998 tasseled cap brightness, greenness and wetness values for six high elevation forest classes. Open overstory classes have < 30% cover, thinned overstory classes have 30–90% cover; closed overstory classes are dominated by sun fleck gaps and other small openings. Classes with different letters have significantly different means based on a Mann–Whitney nonparametric t-test ($\alpha = 0.05$).

Class	Brightness	Greenness	Wetness
Open overstory:	$64.3^A \pm 2.2$	$25.6^A \pm 1.2$	$-19.4^A \pm 0.8$
Understory: fir-dominated	$65.6^a \pm 1.7$	$25.1^a \pm 1.1$	$-20.6^a \pm 0.8$
Understory: deciduous and herbaceous	$61.7^b \pm 5.4$	$26.7^a \pm 2.8$	$-16.7^b \pm 1.5$
Thinned overstory	$56.4^B \pm 2.0$	$23.4^A \pm 1.0$	$-13.2^B \pm 1.1$
Understory: fir-dominated	$55.3^b \pm 2.3$	$25.0^a \pm 1.6$	$-9.6^c \pm 1.0$
Understory: deciduous and herbaceous	$57.1^b \pm 3.0$	$22.2^a \pm 1.3$	$-15.6^{bd} \pm 1.5$
Closed overstory. I.	$45.1^C \pm 3.2$	$16.9^B \pm 1.8$	$-13.5^B \pm 0.9^d$
Fir-dominated overstory	$45.1^c \pm 3.2$	$16.9^b \pm 1.8$	$-13.5^d \pm 0.9$
Closed overstory. II.	$56.7^{AB} \pm 3.2$	$25.9^A \pm 2.0$	$-13.2^B \pm 0.8$
Spruce and spruce-hardwood overstory	$56.7^b \pm 3.2$	$25.9^a \pm 2.0$	$-13.2^{bcd} \pm 0.8$

spruce and spruce/birch sites at the four class level. At the six class level within both the open- and thinned overstory groups, stands with fir understories exhibited different trends than those with deciduous or herbaceous regrowth.

While the open overstory classes and thinned stands with non-fir regrowth had high change magnitudes (indicating considerable change in spectral properties from 1988–1998), they generally had considerably lower mean resultant vector lengths (Table 2). That the mean resultants were higher in sites with lower magnitudes reflected the directional concentration of the CVA angles rather than the amount of change for each class. Specifically, sites with open canopies and a fir understory had a high degree of variability in direction change from 1988–1998 while the other stands, especially closed canopy fir stands, were all changing in a similar direction. These results are supported by the higher directional variance (V) of open and thinned overstory classes vs. those for closed canopy fir and spruce/spruce-hardwood sites.

This pattern was graphically depicted using a polar plot that summarized CVA change by vegetation class (Figures 2 and 3). The circular axis portrays change between the dates in the tasseled cap greenness-wetness plane (θ) while the distance from the origin shows the magnitude of change (Figure 2). In this diagram, the grouping of closed canopy fir sites with low change magnitudes was visually distinguishable from the wider angular distribution and higher magnitude changes of open and thinned sites.
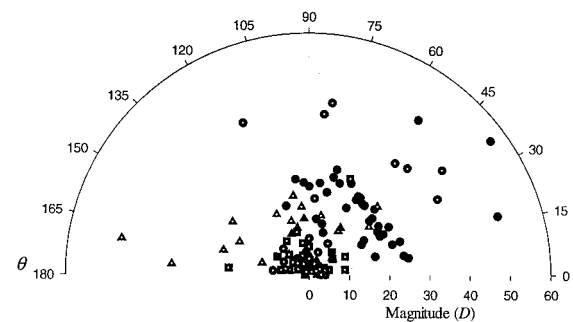

Figure 2. Polar plot of change vector colatitude (angle in tasseled cap wetness-greenness plane) and change magnitude (radii): Open overstory and fir-dominated (●) or deciduous and herbaceous (○) understory; thinned overstory with fir-dominated (▲) or deciduous and herbaceous (△) understory, and closed overstory of predominantly fir (■) or spruce-hardwood dominant (□).

Reflecting the canopy loss of fir and alternate regeneration of young fir or deciduous and herbaceous species (which are captured by tasseled cap wetness), these changes were much more variable than those in Figure 3, which rendered brightness-greenness changes (ϕ). Figure 3, however, underscored the segregation of thinned canopy sites with fir regeneration, which were clustered along the circular axis.

Spatio-temporal variation in tasseled cap-topographic variable relationships

After defining the spectral differences among the various forest classes, we explored the relationships between tasseled cap images and environmental vari-

Table 2. Summary of CVA vector directions by vegetation class. Mean directions are given for colatitude (θ) and colongitude (ϕ) in degrees, class mean change magnitude (D), mean resultant length, and spherical variance (V).

| Class	θ	ϕ	D	R-mean	V
Open Overstory					
Understory: fir-dominated	68.5	208.0	21.8	0.036	0.964
Understory: deciduous and herbaceous	97.2	196.6	16.1	0.059	0.940
Thinned overstory					
Understory: fir-dominated	106.3	146.4	7.6	0.107	0.893
Understory: deciduous and herbaceous	52.6	172.7	13.2	0.060	0.936
Closed overstory. I.					
Fir-dominated overstory	72.2	198.8	5.7	0.185	0.815
Closed overstory. II.					
Spruce and spruce-hardwood overstory	58.0	195.0	7.5	0.060	0.940
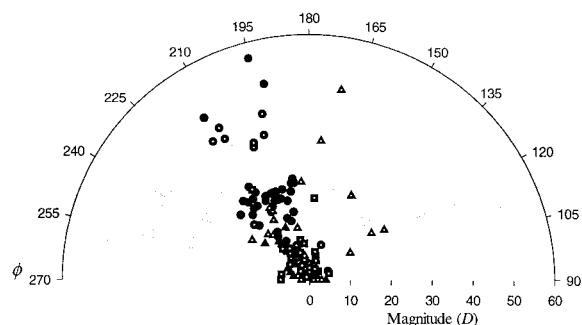
Figure 3. Polar plot of change vector colongitude (angle in tasseled cap brightness-greenness plane) and change magnitude (radii): Open overstory and fir-dominated (●) or deciduous and herbaceous (○) understory; thinned overstory with fir-dominated (▲) or deciduous and herbaceous (△) understory, and closed overstory of predominantly fir (■) or spruce-hardwood dominant (□).

ables to provide an example of how remote sensing techniques utilizing these tools could be used to study and monitor spatial and temporal patterns of mortality and regeneration. We took advantage of the east-west and downslope-upslope chronosequences in adelgid outbreak timing.

Our initial regressions of tasseled cap indices vs. elevation revealed no significant correlations for Mt. Guyot or Mt. LeConte-Mt. Kephart but several significant linear relationships for Clingmans Dome-Mt. Collins (Table 3). Plots of tasseled cap values vs. elevation, however, suggested that the relationships in some cases (especially for LeConte-Kephart) were non-linear (Figure 4). For example, the plot of 1998 greenness vs. elevation for Mt. LeConte suggested a higher order relationship between the variables and thus yielded a low linear coefficient of determination. This non-linearity likely arose because we included lower elevation (1500–1700 m) sites dominated by a mix of red spruce and birch, which may have been spectrally similar to some high elevation sites where Fraser fir has been lost and replaced by mountain ash (*Sorbus americana*) or deciduous shrubs.

Apart from the correlations with elevation, tasseled cap values were significantly related to only a few of the topographic variables. For Mt. Guyot, both brightness and greenness were highly correlated with solar potential, with the strength of the relationships increasing from 1988–1998 (Table 3). For the other mountain groups, few strong and systematic relationships emerged, although solar potential was correlated with brightness in 1998 for both Mt. LeConte-Mt. Kephart and Clingmans Dome-Mt. Collins.

To remove the potentially confounding effects of lower elevation stands, we conducted the same analyses using only stands above 1800 m, thereby limiting our analyses to those stands in the high elevation Fraser fir zone. Of the remaining sites, roughly 70% were open overstory (fir regrowth: 50%, nonfir regrowth: 25%), 15% were closed canopy fir, and 10% were thinned stands. None of the remaining stands were closed canopy spruce-hardwood stands, although several of the thinned stands below 1900 m contained red spruce individuals.

At Mt. Guyot, the only consistent relationships were with solar insolation potential, which was highly correlated with tasseled cap brightness and green-

Table 3. Spectral-topographic relationships (Pearson's *r*) between 1988 and 1998 Landsat tasseled cap transforms and elevation. Elevation range of sites shown in parentheses.

Site	Band	Elevation	Slope	Curvature	Solar pot.	Flow
Clingman–Collins	Bright_88	**−0.30***	0.03	**−0.25***	−0.02	**0.34***
(1533–1999 m)	Bright_98	0.17	−0.11	−0.19	**0.36***	0.07
	Green_88	**−0.46***	0.08	**−0.29***	**−0.24***	0.13
	Green_98	0.04	−0.06	**−0.26***	0.23	0.06
	Wet_88	0.16	0.16	0.08	−0.18	−0.08
	Wet_98	**−0.52****	−0.10	0.02	**−0.30***	0.06
LeConte–Kephart	Bright_88	0.01	−0.06	−0.10	0.07	−0.04
(1549–1988 m)	Bright_98	0.15	−0.14	0.10	**0.24***	−0.15
	Green_88	−0.08	−0.14	−0.13	0.05	−0.04
	Green_98	0.06	−0.18	0.13	0.19	−0.19
	Wet_88	−0.20	−0.06	−0.16	−0.10	**0.26***
	Wet_98	−0.18	0.01	0.00	−0.17	0.01
Guyot	Bright_88	0.17	0.05	0.12	**0.58*****	0.01
(1803–2006 m)	Bright_98	0.01	0.11	0.06	**0.62*****	−0.06
	Green_88	0.10	−0.02	0.09	0.36	0.08
	Green_98	0.05	0.07	0.05	**0.63*****	−0.04
	Wet_88	0.17	−0.12	−0.04	−0.20	−0.13
	Wet_98	0.30	−0.34	−0.03	−0.02	−0.05

Significance levels: *0.01 < *p* < 0.05; **0.001 < *p* < 0.01; *** *p* < 0.001.

Table 4. Correlations between Landsat tasseled cap transforms (1988 and 1998) and environmental variables. Sites are only those in the Fraser fir zone (> 1800 m asl).

Site	Band	Elevation	Slope	Curvature	Solar pot.	Flow
Clingman–Collins	Bright_88	0.01	**0.31***	−0.09	0.08	0.15
	Bright_98	**0.44*****	0.13	−0.16	**0.44*****	−0.01
	Green_88	−0.14	**0.38****	−0.05	−0.16	0.09
	Green_98	**0.30***	0.19	−0.18	**0.37****	0.05
	Wet_88	−0.07	0.05	0.11	**−0.29***	−0.10
	Wet_98	**−0.49*****	−0.08	0.14	**−0.34****	−0.01
LeConte–Kephart	Bright_88	**0.41****	**−0.34***	−0.04	0.30	−0.08
	Bright_98	**0.58*****	**−0.40***	0.14	**0.47*****	−0.16
	Green_88	**0.39***	**−0.54*****	−0.03	**0.33***	0.02
	Green_98	**0.52*****	**−0.36***	0.25	**0.43****	−0.20
	Wet_88	−0.15	**−0.34***	−0.03	0.02	0.25
	Wet_98	**−0.31***	**0.32***	−0.01	−0.31	−0.02
Guyot	Bright_88	0.17	−0.05	0.12	**0.58*****	0.01
	Bright_98	0.01	0.11	0.06	**0.62*****	−0.06
	Green_88	−0.10	−0.02	0.09	**0.36***	−0.08
	Green_98	0.05	0.07	0.05	**0.63*****	−0.04
	Wet_88	−0.17	−0.12	−0.04	−0.26	−0.13
	Wet_98	0.30	−0.33	−0.03	−0.02	−0.05

Significance levels: *0.01 < *p* < 0.05; **0.001 < *p* < 0.01; *** *p* < 0.001.
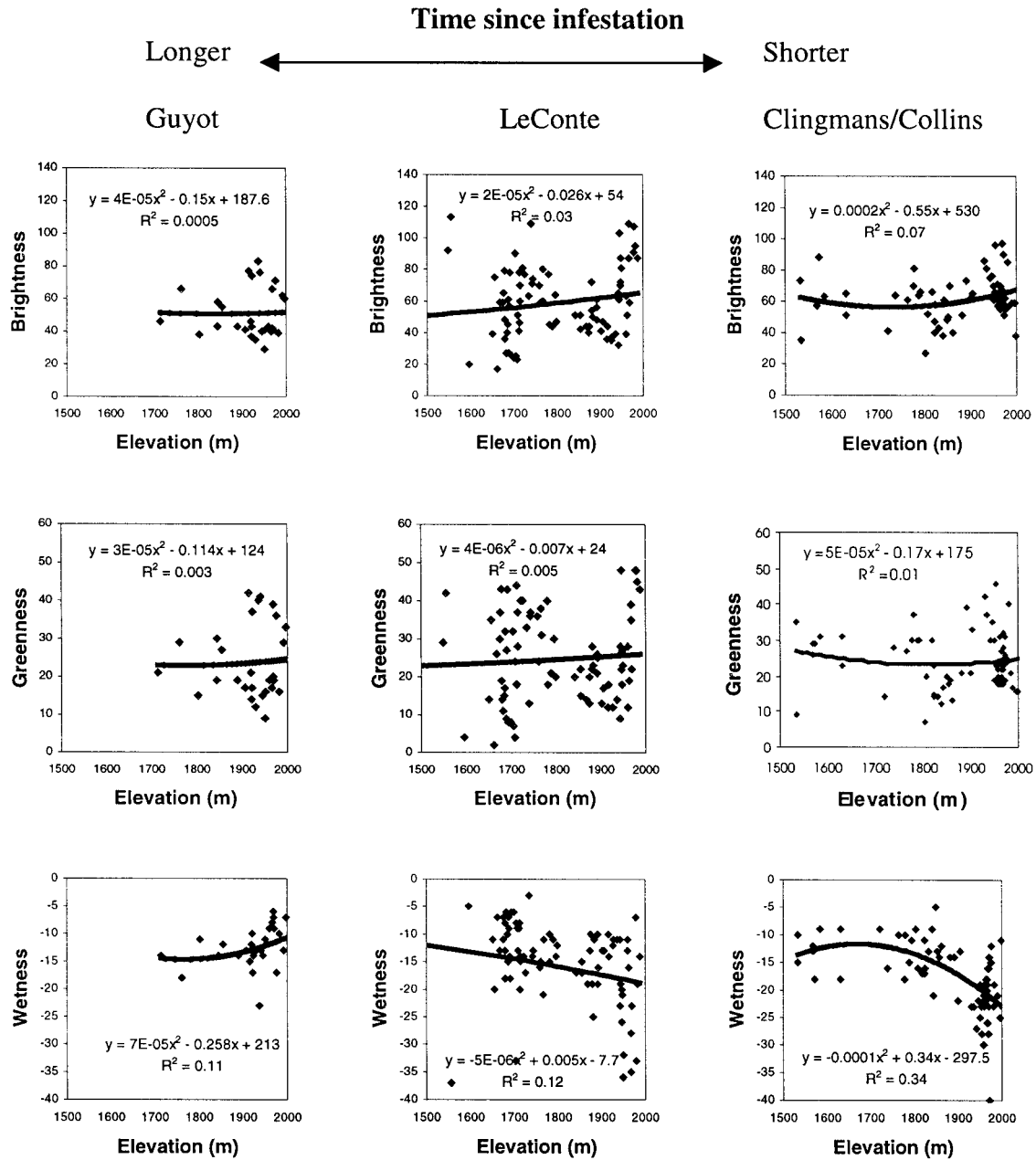
Figure 4. Spatially-stratified east-west chronosequence regression analysis of 1998 Landsat TM tasseled cap transform bands (brightness, greenness, and wetness) and DEM-derived elevation.

ness (Table 4). These correlations suggest associations between: (a) open canopy stands and high solar potential (e.g., south-facing slopes) and (b) closed canopy fir stands and low solar potential (e.g., north-facing slopes). Because of the longer time since infestation on Mt. Guyot, some of the larger firs that composed the closed canopy fir stands appeared to be post-infestation regeneration, suggesting that establishment, growth and survival of fir following the wave of adelgid infestation in the 1960–1970s may have been favored on protected exposures.

For the central mountain group (LeConte–Kephart), elevation was significantly related to tasseled cap brightness and greenness in both years as

well as wetness in 1998. Given the relationships between these variables and the forest classes (Table 1), the positive relationship between brightness and elevation suggested a more open overstory near the crests. This finding was consistent with the greater importance of fir at the highest elevations (1950–2000 m) in pre-infestation stands while thinned stands, which often contained a number of surviving red spruce, tended to occur around 1800–1900 m. In 1988, when mortality was peaking at Mt. LeConte, tasseled cap brightness, greenness and wetness were significantly associated with slope, suggesting that forest community distribution at this time was structured by slope steepness. However, as with Mt. Guyot, the strongest relationships between tasseled cap values and topographic variables in 1998 (apart from elevation) were with solar potential. The nature of the relationships again suggests, though not as strongly, that fir is faring better on protected slopes.

In the most recently affected area (Clingmans Dome/Mt. Collins), elevation showed no relationship to tasseled cap indices in 1988. Given that adelgid-caused mortality was still in an early phase on the slopes above 1800 m at Clingmans Dome at this time and that many of our sites would have contained closed fir forest, these results confirmed our expectation that reflectance values before fir decline did not vary greatly with elevation. The inverse relationship between wetness and solar potential in 1988 supported the conclusion that most of the stands were closed fir forest in that higher wetness values are logically the result of low solar potential if vegetation type is similar. Conversely, no such relationship existed for the other mountains because the effects of forest decline on wetness were already well established prior to the 1988 image. By 1998, wetness, greenness and brightness were all related to elevation (Table 4), indicating that once fir began to decline in the 1990s, the extent of decline and the subsequent regeneration were shaped by elevation. Finally, as with the other two mountain groups, tasseled cap indices were significantly correlated with solar potential in 1998.

As a visual means for conveying the geographic variation in change vectors, we created a vane plot and overlaid it on a location map (Figure 5). The symbols, similar to weather vanes, portray the change vector summary statistics for each mountain, including spherical direction variance (vane base), CVA magnitude (D) (vane length), and mean direction in the wetness-greenness plane (orientation of vane). The implications of these data are described below.

Within-forest class trends

Finally, to examine change properties within the mortality/regeneration classes, we performed a series of correlations between the CVA variables and the topographic variables for all sites belonging to each vegetation class in 1998. All thinned overstory sites were pooled as a group as were all closed overstory sites owing to sample size. The results of these analyses indicated that the amount and direction of change for sites in the same classes were often related to abiotic conditions, suggesting different successional trajectories on sites with different environmental settings (Table 5). For example, change magnitudes were highest at high elevations for the open and thinned overstory plots, especially for the open overstory plots with non-fir regrowth. This finding is consistent with the timing of the images and the downslope-upslope chronosequence of adelgid effects; that is, mortality was still occurring at the highest elevations between 1988 and 1998, resulting in greater change magnitudes. The direction of spectral change from 1988–1998 also differed for thinned plots as a function of elevation.

With respect to the other topographic variables, change magnitude was:
– low for high slope sites in thinned and closed overstory plots;
– high for high slope sites in open overstory, fir plots; and
– high for sites with high solar potential (exposed slopes).

Change direction along the wetness/greenness plane, θ, and/or along the greenness/brightness plane, ϕ was shaped by:
– slope angle and curvature for thinned sites,
– slope curvature and slope position for open overstory, non-fir understory sites, and
– solar potential, for open overstory, fir understory plots.

Finally, it is worth noting that there was little segregation of change variables by topographic features for the closed overstory plots. This latter finding, when coupled with our earlier finding that closed overstory plots generally exhibited little overall change (Table 2), suggests that closed overstory plots were not significantly changing nor did they seem to be changing in any systematic way.
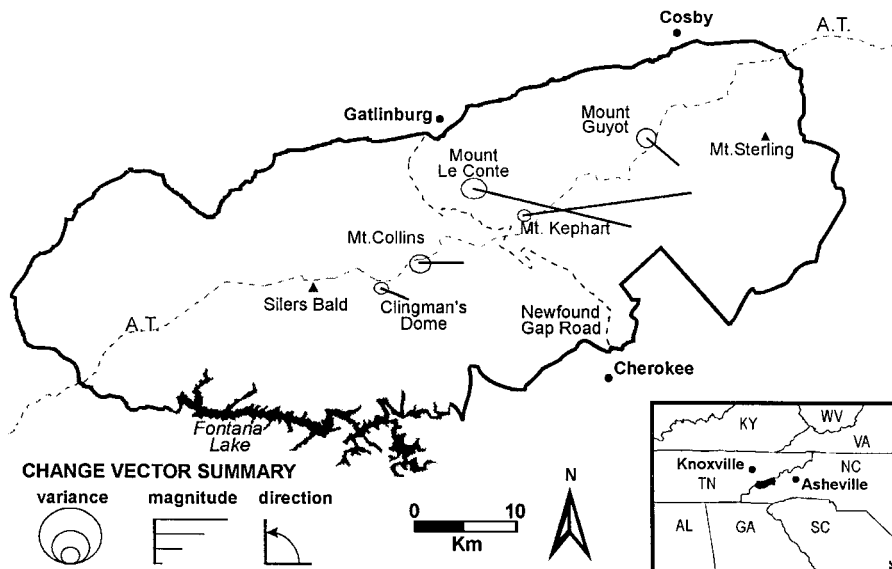
Figure 5. Study area map with vane plot summary change vectors for 1988–1998 Landsat TM for five Great Smoky Mountain sites (vane base diameter signifies directional variance, vane length is vector mean resultant magnitude, and direction is mean angle θ wetness-greenness).

Discussion

Vegetation patterns

Our initial hypothesis was that vegetation patterns in the wake of adelgid-caused forest declines would be a function of initial fir densities (which were related to elevation), time since infestation (captured by east-west and downslope-upslope gradients) and the response of vegetation to environmental conditions. Each element of this hypothesis was supported in our analysis. The influence of initial fir densities and time since infestation were especially apparent in the analyses of elevation effects by mountain range and were underscored by the change vector analyses. For example, we identified strong relationships between elevation and tasseled cap values for both Mt. LeConte–Mt. Kephart and Clingmans Dome–Mt. Collins (Table 4). Given that tasseled cap values successfully discriminated open vs. thinned vs. closed sites (Tables 1 and 2), these associations apparently captured the upslope movement of adelgid effects. On the central mountain group, sites at lower elevations were already experiencing fir declines in the late 1970s and early 1980s while the effects were delayed until later in the 1980s at higher elevations. The lower wetness values for high elevation sites can be inferred as a result of a more open canopy. Higher values at low elevations reflect both the increased presence of species other than fir (especially red spruce

and yellow birch) as well as a longer period of recovery since adelgid-caused declines, corroborating the hypothesized upslope migration path of adelgid infestation.

An equally strong, but delayed, relationship holds for the 1988 and 1998 tasseled cap values at Clingmans Dome/Mt. Collins (Table 4). On Mt. Collins, which includes most of the lower elevation areas of the Clingmans–Collins massif, the adelgid had established in significant numbers in the mid-1980s. Mortality did not peak on the higher elevation slopes of Clingmans until the 1990s. The very top of Clingmans Dome still retained some stands of mature fir in 2000; hence, these high elevation sites exhibited low greenness (Figure 4). Elevation was thus significantly correlated with brightness and greenness (which primarily separate mature fir stands from other vegetation types) in 1988 when the adelgid was just beginning to affect this area, and dense pure fir stands were limited to the relatively unaffected areas above 1800 m. However, elevation was strongly correlated with wetness (and thus openness) in 1998, a reflection of the upslope wave of adelgid-caused mortality. In contrast, dieback had occurred as much as one to two decades before the 1998 surveys at even the highest elevations of Mt. Guyot, as is evidenced by the abundance of mature individuals of all species (including mountain ash and yellow birch > 15–25 cm dbh) along the elevation gra-

Table 5. Pearson correlations between CVA magnitude (*D*), linear normalized colatitude (*θ*) and colongitude (*φ*) and elevation and derivative topographic variables for sites above 1800 m. Thinned and closed overstory classes pooled to preserve sample sizes.

Class	CVA	Correlations				
		Elevation	Slope	Curvature	Solar	Flow
Open overstory	*D*	**0.27***	**0.30***	−0.06	0.148	−0.23
Fir-dominated understory	*θ*	0.17	−0.05	−0.04	**0.315****	−0.112
	φ	0.21	0.02	−0.10	**0.315****	−0.108
Open overstory	*D*	**0.80******	−0.15	**0.50****	**0.71******	**−0.43****
Deciduous and	*θ*	0.24	0.03	**0.35***	0.10	−0.05
herbaceous understory	*φ*	0.33	−0.16	**0.38***	0.29	**−0.52****
Thinned overstory	*D*	**0.43***	**−0.46***	−0.30	**0.51****	−0.23
	θ	**0.63****	**−0.55*****	**−0.57*****	−0.26	−0.03
	φ	**0.86******	**−0.57****	**−0.43***	0.37	−0.18
Closed overstory	*D*	−0.25	**−0.36***	0.02	0.20	−0.18
	θ	0.11	0.28	0.06	−0.12	**0.53****
	φ	0.27	0.35	−0.12	−0.17	−0.15

Significance levels: *$0.10 < p < 0.05$; **$0.01 < p < 0.05$; ***$0.001 < p < 0.01$; ****$p < 0.001$.

dient. As a result, there was no obvious relationship between elevation and any of the tasseled cap indices.

The nonlinearity of the relationship between elevation and tasseled cap values for some areas (Figure 4) further supports these results in that it is related to the interrelations among the elevation gradient, species niches and the dispersal of the adelgid. The parabolic nature of the relationship is especially evident for Mt. LeConte–Mt. Kephart and occurred because fir dieback was most recent at the highest elevations. The replacement of mature fir stands by non-fir species such as blackberry led to a spectral signature similar to that of downslope areas containing a large deciduous component (e.g., yellow birch).

The CVA data provided us with a unique perspective that substantiated the hypothesized mortality and regeneration patterns arising from a temporal gradient of infestation. The east-west chronosequence developed by regression analysis (Table 4) and visualization of CVA (Figure 5) suggests that along a continuum, or possibly cycle, of adelgid disturbance, the patterns of mortality and regeneration, can be spectrally distinguished. For example, Mt. Guyot, site of the earliest adelgid infestation, exhibited moderate variation of CVA direction but the lowest greenness-wetness direction change. This is a consequence of the timing of infestation, as fir mortality here occurred prior to the date of the first image (1988). For Mt. Guyot, the images are almost strictly capturing regeneration, pri-

marily that for thinned and open overstory stands that previously were in continuous fir.

In comparison, Mt. LeConte and Kephart in the central Smokies exhibited very large change magnitudes, owing to more recent fir mortality that struck elevations near the hardwood-conifer ecotone in the early and mid-1980s and peaked at higher elevations in the late 1980s. Regeneration at these sites, which is highly patchy, has been occurring throughout (and even slightly prior to) the interval of these images, leading to high magnitudes of change. In addition, both Kephart and LeConte show similar directional vectors, suggesting a synchrony in regeneration timing. Finally, the Clingmans Dome and Mt. Collins sites are the most recently affected areas, and both show low variance and moderate magnitudes. Because these sites have so recently undergone fir mortality, regeneration in many sites is just beginning. Thus, high magnitudes are not to be expected and regeneration paths are less clearly evidenced.

Within the landscape-level context of variations in disturbance timing and length of recovery, the reflectance properties (Table 4) and forest classes (A1, A2, B1, B2, C1, C2) (Tables 2 and 5) were related to topographically-derived variables that served as proxies for site conditions. In most cases, significant relationships between tasseled cap values and environmental variables were stronger:
 – in 1998 than 1988, and

– when only sites above 1800 m were examined. Both of these results have straightforward interpretations. In the first case, a strengthening of vegetation-environment relationships is expected because most of the sites are in the process of recovering from extensive mortality. Little difference in reflectance for sites varying in abiotic conditions would be expected when all sites are experiencing catastrophic declines (especially given the amount of variation introduced by elevation-related differences in the timing of decline). However, the nature of the regrowth (e.g., fir vs. blackberry) after ten additional years of recovery would be expected to be more strongly tied to conditions such as solar potential, slope and curvature. The relationships for sites above 1800 m are likely stronger for a similar reason. At sites below this level, post-adelgid succession proceeded in the presence of previously established vegetation (e.g., spruce and fir), which could act to mediate the importance of environmental variables. When the sites were limited to just relatively pure fir stands, the removal of nearly the entire canopy accentuated differences in site environment related to topographically-controlled variables.

The CVA added insight into the dynamic behavior of these forest classes not normally provided by vegetation-environment correlations (Table 5). Specifically, sites even within classes exhibited differences in the amount (i.e., magnitude) and direction of change depending on their abiotic conditions.

Change vector analysis approach

The remote sensing approach taken in this study allowed for the testing of hypotheses across multiple scales. Specifically, the analysis of Fraser fir stands at the site-level, on individual mountains, and across the Smoky Mountain range was more effective with the synoptic scale and multitemporal perspective afforded by satellite imagery. The integration of topographic variables in a geographic information system also provided the vital data for associating spectral changes to abiotic conditions. The difficulty of terrain to field-based measurements across wide areas provided an additional impetus for pursuing a remote sensing approach. The methodology was also complicated by topographic effects that make remote sensing applications in many mountain environments challenging (e.g., the need to normalize the images for slope angle, orientation, and shadowing conditions; Allen 2000). Both these limitations were generally overcome by preprocessing techniques.

Identifying the spatial and temporal scales of earth surface variation has been a significant research problem in remote sensing and geographic information science (Davis et al. 1991), and the importance of including a landscape-level perspective in forest management and conservation plans is now recognized (e.g., Kupfer 1995). Our identification and quantification of the spatial processes of Fraser fir mortality and regeneration would have been much more difficult in the absence of the technologies of GIS, digital image processing, and global positioning system. Though angular measurement has been illustrated before using CVA, such as for input to image classification (Cohen & Fiorella 1998), this project illustrates a CVA approach for analyzing spectral changes in biophysically meaningful indices (tasseled cap bands) and subsequently to highlight changes in relation to environmental variables. While transformations of radiometric and atmospheric conditions between image dates remain a concern as they have for more than a decade of change detection (Walsh 1989), this research provides an example of an alternative change detection technique and an improvement in the use of the longstanding CVA technique.

The correlation of CVA and topographic variables, and the significant differences in vectors across vegetation classes, illustrates the utility of spherical geometry for monitoring coniferous forests. Tasseled cap bands were easily adapted to the CVA approach because of their data compression and a simple 3-band dimensionality for Euclidean geometry. Such an application of spherical statistics in conjunction with CVA and GIS-derivative variables provides a potential area for further research exploration. The general approach to identifying spectral signatures in remote sensing also has the potential for analogous temporal signatures in conjunction with CVA. The tasseled cap bands, which themselves are based upon on temporal patterns of crop phenology, provide an example for forestry and land cover change applications. With a longer time series of imagery or controlled experiment, temporal patterns of spectral response could be derived in CVA-space diagrams, and new multitemporal, multispectral indices for ecological processes could be derived. Additional research on the approach could evaluate such use of CVA with longer and more detailed image time series or the analysis of vegetation phenology or interannual variation.

Acknowledgements

References

Allen, T. R. 2000. Topographic normalization of Landsat Thematic Mapper data in three mountain environments. Geocarto Int. 15: 13–19.

Allen, T. R. & Kupfer, J. A. 2000. Application of spherical statistics to change vector analysis of Landsat data: Southern Appalachian spruce-fir forests. Remote Sensing Environ. (in press).

Alsop F. J. & Laughlin, T. F. 1991. Changes in the spruce-fir avifauna of Mt. Guyot Tennessee 1967-1985. J. Tenn. Acad. Sci. 66: 208–210.

Balch, R. E., Clarke, J. & Bonga, J. M. 1964. Hormonal action in products of tumors and compression wood in *Abies balsamea* (L.) Mill. by an aphid (*Adelges piceae*). Nature 202: 721–722.

Bonneau, L. R., Shields, K. S. & Civco, D. L. 1999. A technique to identify changes in hemlock forest health over space and time using satellite image data. Biol. Invas. 1: 269–279.

Brockhaus, J. A., Khorram, S., Bruck, R. I., Campbell, M. V. & Stallings C. 1992. A comparison of Landsat TM and SPOT HRV data for use in the development of forest defoliation models. Int. J. Remote Sensing 13: 3235–3240.

Buchheim, M. P., Maclean, A. L. & Lillesand, T. M. 1985. Forest cover type mapping and spruce budworm defoliation detection using simulated SPOT imagery. Photogram. Engin. Remote Sensing 51: 1115–1122.

Busing, R. T., White, P. S. & MacKenzie, M. D. 1993 Gradient analysis of old spruce-fir forests of the Great Smoky Mountains circa 1935. Can. J. Bot. 71: 951–958.

Cohen, W. B. & Fiorella, M. 1998. Comparison of methods for detecting conifer forest change with thematic mapper imagery. Pp. 89–102. In: Lunetta, R. S. & Elvidge, C. D. (eds), Remote sensing change detection: environment monitoring methods and applications. Ann Arbor Press, Chelsea, Michigan.

Collins, J. B. & Woodcock, C. E. 1994. Change detection using the Gramm-Schmidt transformation applied to mapping forest mortality. Remote Sensing Environ. 50: 267–279.

Collins, J. B. & Woodcock, C. E.. 1996. An assessment of several linear change detection techniques for mapping forest mortality using multitemporal Landsat TM data. Remote Sensing Environ. 56: 66–77.

Crist, E. P & Cicone, R. C. 1984. Application of the tasseled cap concept to simulated thematic mapper data. Photogram. Engin. Remote Sensing 50: 343–352.

Davis, F. W., Quattrochi, D. A., Ridd, M. K., Lam, N. S-N, Walsh, S. J., Michaelsen, J. C., Franklin, J., Stow, D. A., Johannsen, C. J. & Johnston C. A. 1991. Environmental analysis using integrated GIS and remotely sensed data: Some research needs and priorities. Photogram. Engin. Remote Sensing. 57: 689–697.

DeSelm, H. R. & Boner, R. R. 1984. Understory changes in spruce-fir during the first 16–20 years following the death of fir. In: White, P. S. (ed.), The Southern Appalachian spruce-fir ecosystem: its biology and threats. National Park Service Southeast Region, Research/Resources Management Report SER-71, Atlanta, GA.

Eckhardt, D. W., Verdin, J. P. & Lyford, G. R. 1990. Automated update of an irrigated lands GIS using SPOT HRV imagery. Photogram. Engin. Remote Sensing 56: 1515–1522.

Ekstrand, S. 1989. The possibilities of assessing moderate damages on Norway spruce using Landsat TM data and ancillary stand information in a GIS environment. Proceedings, IGARSS '89 Symposium. Vancouver, Canada, 1553–1557.

Fisher, N. I. 1993. Statistical analysis of circular data. Cambridge University Press, Cambridge.

Fisher, N. I., Lewis, T. & Embleton, B. J. J. 1987. Statistical analysis of spherical data. Cambridge University Press, Cambridge.

Franklin, S. E. & Raske, A. G. 1994. Satellite remote sensing of spruce budworm forest defoliation in western Newfoundland. Can. J. Remote Sensing 20: 37–48.

Hadley, K. S. & Veblen, T. T. 1993. Stand response to western spruce budworm and Douglas-fir bark beetle outbreaks, Colorado Front Range. Can. J. Forest Res. 23: 479–491.

Hall, F. G., Strebel, D. E., Nickeson, J. E. & Goetz, S. J. 1991. Radiometric rectification: Toward a common radiometric response among multi-date, multi-sensor images. Remote Sensing Environ. 35: 11–27.

Hay, R. L., Eagar, C. C. & Johnson, K. D. 1978. Fraser fir in the Great Smoky Mountains National Park: its demise by the balsam woolly aphid (*Adelges piceae* Ratz.). Contract Report, USDI National Park Service, SE Region, Atlanta, GA.

Jenkins, J. C., Aber, J. D. & Canham, C. D. 1999. Hemlock woolly adelgid impacts on community structure and N cycling rates in eastern hemlock forests. Can. J. Forest Res. 29: 630–645.

Jensen, J. R., Rutchey, K., Koch, M. S. & Narumalani, S. 1995. Inland wetland change detection in the Everglades Water Conservation Area 2A using a time series of normalized remotely sensed data. Photogram. Engin. Remote Sensing 61: 199–209.

Joria, P. E., Ahearn, S. C. & Connor, M. 1991. A comparison of the SPOT and Landsat Thematic Mapper satellite systems for detecting gypsy moth defoliation in Michigan. Photogram. Engin. Remote Sensing 57: 1605–1612.

Kupfer, J. A. 1995. Landscape ecology and biogeography. Progr. Phys. Geogr. 19: 18–34.

Kupfer, J. A., Allen, T. R. & Cairns, D. M. Spatial aspects of mortality and regeneration in Fraser fir ecosystems following introduction of the balsam woolly adelgid. In review, Biol. Invas.

Luther, J. E., Franklin, S. E., Hudak, J. & Meades, J. P. 1997. Forecasting the susceptibility and vulnerability of balsam fir stands to insect defoliation with Landsat Thematic Mapper data. Remote Sensing Environ. 59: 77–91.

McCullough, D. G., Marshal, L. D., Buss, L. J. & Kouki, J. 1996. Relating jack pine budworm damage to stand inventory variables in northern Michigan. Can. J. Forest Res. 26: 2180–2190.

Muchoney, D. M. & Haack, B. N. 1994. Change detection for monitoring forest defoliation. Photogram. Engin. Remote Sensing 60: 1243–1251.

Mukai, Y., Sugimura, T., Watanabe, H. & Wakamori, K. 1987. Extraction of areas infested by pine bark beetle using Landsat MSS data. Photogram. Engin. Remote Sensing 53: 77–81.

Nelson, R. F. 1983. Detecting forest canopy change due to insect activity using Landsat MSS. Photogram. Engin. Remote Sensing 49: 1303–1314.

Nicholas, N. S., Eagar, C. C. & Peine, J. D. 1999. Threatened ecosystem: High elevation spruce-fir forest. In: Peine, J. D. (ed.), Ecosystem management for sustainability. Lewis Publishers, Boca Raton, FL.

Nicholas, N. S., Zedaker, S. M. & Eagar, C. C. 1992. A comparison of overstory community structure in three southern Appalachian spruce-fir forests. Bull. Torrey Bot. Club 119: 316–332.

Noss, R. F., LaRoe, E. T. & Scott, J. M. 1995. Endangered ecosystems of the United States: a preliminary assessment of loss and degradation. U.S. Dept. of the Interior, National Biological Service, Washington, D.C.

Orwig, D. A. & Foster, D. R. 1998. Forest response to the introduced hemlock woolly adelgid in southern New England, USA. J. Torrey Bot. Soc. 125: 60–73.

Pauley, E. F. & Clebsch, E. E. C. 1990. Patterns of *Abies fraseri* regeneration in a Great Smoky Mountains spruce-fir forest. Bull. Torrey Bot. Club 117: 375–381.

Pyle C. 1985. Vegetation disturbance history of Great Smoky Mountains National Park: an analysis of archival maps and records. U.S. Department of the Interior, National Park Service, Research/Resources Management Report SER-77, Southeast Regional Office Atlanta, GA.

Rabenold, K. N., Fauth, P. T. & Parker, P. G. 1998. Response of avian communities to disturbance by an exotic insect in spruce-fir forest of the Southern Appalachians. Cons. Biol. 12: 177–189.

Radeloff, V. C., Mladenoff, D. J. & Boyce, M. S. 1999. Detecting jack pine budworm defoliation using spectral mixture analysis: Separating effects from determinants. Remote Sensing Environ. 69: 156–169.

Rock, B. N., Vogelmann, D. L., Williams, A. E. & Hoshizaki, T. 1986. Remote detection of forest damage. BioScience 36: 439–445.

Royle, D. D. & Lathrop, R. G. 1997. Monitoring hemlock forest health in New Jersey using Landsat TM data and change detection techniques. Forest Sci. 42: 327–335.

Smith, G. F. & Nicholas, N. S. 1998. Patterns of overstory composition in the fir and fir-spruce forests of the Great Smoky Mountains after balsam woolly adelgid infestation. Am. Midland Nat. 139: 340–352.

Smith, G. F. & Nicholas, N. S. 2000. Size- and age-class distributions of Fraser fir following balsam woolly adelgid infestation. Can. J. Forest Res. 30: 948–957.

Swetnam, T. W. & Lynch, A. M. 1993. Multicentury, regional-scale patterns of western spruce budworm outbreaks. Ecol. Monogr. 63: 399–424.

Walsh, S. J. 1989. User considerations in landscape characterization. Pp. 35–43. In: Goodchild M. & Gopal S. (eds), Accuracy of Spatial Databases. Taylor and Francis, New York.

Whittaker, R. H. 1956. Vegetation of the Great Smoky Mountains. Ecol. Monogr. 26: 1–80.

Yuan, D. & Elvidge, C. D. 1996. Comparison of relative radiometric normalization techniques. ISPRS J. Photogram. Remote Sensing, 51: 117–126.